Watermarking on Compressed Image: A New Perspective

Santi P. Maity[1] and Claude Delpha[2]
[1]Bengal Engineering and Science University, Shibpur
[2]Laboratoire des Signaux et Systemes, Universite Paris, SUPELEC,CNRS
[1]India
[2]France

1. Introduction

Watermarking is highly demanding in recent times for the protection of multimedia data in network environment from illegal copying, violation of copyright, authentication etc (Hartung & Kutter,1999), while compression of multimedia signals is essential to save storage space and transmission time. Hence, it is needless to mention the importance of watermarking on compressed data. However, the working principles of watermarking and compression seem to be different as perceptual data coding removes inherent redundancy during compression. On the other hand, watermarking uses this redundancy space for making data embedding imperceptible. As a matter of fact, watermarking on compressed data becomes more challenging, and many solutions come out as an optimization problem in the form of joint watermarking and compression (JWC). Moreover, the other requirement is that watermarking process should not increase bit rate for the compressed data to a large extent while satisfying high value of document-to-watermark ratio (DWR) and watermark decoding reliability. Over and above, it is desirable that watermarking algorithm must be compatible with ease of integration with the existing compression framework, for example, JPEG and JPEG 2000 compression for digital images.

The objective of this chapter is to first look into the fundamental problems in watermarking on compressed data followed by robust and efficient algorithm design. The readers would understand stepwise movement for the choice of different tools and techniques to develop an integrated algorithm to meet certain well-defined objectives. One such objective considered here is to develop high DWR and low bit error rate (BER) watermarking system with moderate payload and without much increase in file size of the compressed watermarked data. This can be accomplished by using error correction code (ECC) intelligently through the creation of virtual redundancy space. In other words, the flexibility for data embedding lost due to quantization operation may be regenerated by applying channel coding scheme directly on the host compressed data, instead of applying it on watermark signal as is done in the conventional watermarking system. It should also be considered that the so called created redundancy should not increase much the file size of the compressed watermarked data which is the primary goal of compression operation.

The rest of the chapter is organized as follows: Section 2 makes a brief literature review on related works and their limitations followed by the scope of the present work. A general outline for new algorithm design of watermarking on compressed data is then highlighted in Section 3. Section 4 presents proposed watermarking method, while performance analysis is done in Section 5. Finally conclusions are drawn in Section 6 along with scope of the future works.

2. Review of related works, limitations and scope of the work

In this section, we present a brief literature review for watermarking on compressed data with an objective to discuss their merits, limitations and finally scope of the proposed work.

2.1 Related works and limitations

Some watermarking algorithms work entirely on the compressed domain such as JPEG-to-JPEG (J2J) watermarking (Wong, 2000; Wong2001). Robust watermarking scheme is proposed in (Wong & Au, 2002) using iterative spread spectrum technique (SST) in JPEG images. These methods embed different amount of watermark bits into JPEG images while maintaining good visual quality of the watermarked JPEG images. Huang et al (Huang et al., 2007) propose an effective watermark embedding method for JPEG image which can resist high compression attack and retains a good image quality. The algorithm consists of three parts, searching for the optimal embedding position, proper embedded value and the embedded/extracted processing based on quantization index modulation (QIM). Elbasi (Elbasi, 2007) propose a robust MPEG video watermarking in wavelet domain by embedding a pseudo random sequence in MPEG-1 using two bands (LL-low low and HH-high high). They show experimentally that for one group of attacks (i.e. JPEG compression, Gaussian noise, resizing, lowpass filtering, rotation and frame dropping), the correlation with the real watermark is higher than the threshold in the LL band, and for another group of attacks (i.e. cropping, histogram equalization, contrast adjustment and gamma correction), the correlation with real watermark is higher than the threshold in the HH band.

Taniguchi (Taniguchi, 2005) proposes a method that provides robustness against scaling for watermarked MPEG content using a pseudo-random sequence of block patterns and a tiled structure. Detection of the watermark information is based on a cross-correlation between the watermarked content and the watermark pattern. Basically the scaling change is detected by observing the auto-correlation peaks generated by the tiled structure. Allatar etal (Allatar at el., 2003) propose a novel watermarking method for low bit rate video that is compressed according to the advanced simple profile of MPEG-4. A simple spread spectrum watermark was embedded directly to the MPEG-4 bit-streams. A synchronization template was employed to combat cropping, scaling, and rotation. A gain control algorithm adjusts the local strength of the watermark depending on local image characteristics, in order to maximize watermark robustness and to minimize the impact on the quality of the video. He et al (He et al., 2002) propose an object based watermarking solution for MPEG4 video authentication. Nakajima et al. (Nakajima et al.,2005) proposed a high capacity data hiding method in MPEG domain utilizing the idea of zero run-level encoding.

Embedding of watermark information on compressed data needs partial or full decoding depending on the domain where the watermark would be embedded in least significant bits

(LSB) of the levels of variable-length codes (VLC) in MPEG stream (Langelaar, 2000), and the same for the appended bits of certain pairs of AC coefficients of JPEG data (Fridrich, 2004), are made to match the watermark bit. The approach in (Langelaar, 2000) is effective but is lossy, too predictable and requires Huffman decoding of the JPEG file, while (Fridrich, 2004) is an adaption of (Langelaar, 2000) to JPEG. A fragile but lossless and file preserving watermarking algorithm is proposed in (Mobasseri, 2005) that is applicable to any entropy coded compression stream, provided that the total code space is not used. Inter-block correlation of the selected DCT coefficients for JPEG compressed data, by adding or subtracting an off-set to the mean value of the neighboring DCT coefficients, are also used in (Choi, 2000) and in (Luo, 2002) to embed watermark.

An achievable region of quantization (or compression) rate and embedding rate was developed in (Karakos, 2003) in the case of private watermarking, Gaussian host signals, and a fixed Gaussian attack. In (Maor,2004), the attack-free public version of the problem was treated, both for the finite and continuous alphabet cases. In (Maor,2005) the best trade-offs among the embedding rate, compression rate, and quantization distortion were studied from an information theoretic perspective for public watermarking in the case of a finite alphabet and a fixed memoryless attack channel. Wu et al (Wu et al.,2005) maximizes robustness of watermark decoding against additive white Gaussian noise (AWGN) in the context of JWC. They first investigate optimum decoding of a binary JWC system, and demonstrate by experiments the distortion-to-noise (DNR) region of practical interest. The minimum distance (MD) decoder achieves performance comparable to that of the maximum likelihood decoder. In addition, it offers advantages of low computation complexity and is also independent of the statistics of the host signal.

On summarization of the review works, it is observed that watermark embedding in the bitstream domain (Mobasseri, 2005) is fragile and requires re-encoding at alternate bit rates. On the other hand, JWC works reported in (Wu, 2005) are mostly ad hoc and put primary focus on quantization (or compression) rate and embedding rate. The other J2J works reported in (Langelaar, 2000; Fridrich, 2004; Choi, 2000; Luo, 2002) show much performance degradation both in DWR and the reliability of the watermark decoding against AWGN, with the increase of the compression rate. Works reported in (Karakos, 2003; Maor, 2004; Maor, 2005) consider trade-off aspects of embedding rate, compression rate, quantization distortion but suffer from overhead problem, large size in code book, lack of involvement of real life host data. These drawbacks create a pressing demand for practical implementation of watermarking algorithm on real life compressed host image. Another important aspect of watermarking on the compressed data, to the best of our knowledge, is possibly unexplored; how to increase simultaneously DWR and watermark decoding reliability i.e. low bit error rate (BER) for the given compression rate (determines the size of the embedding space) with moderate watermark payload and at the same time the size (bit rate) of the compressed watermarked data does not change much.

2.2 Scope of the work

The objective here is to develop an algorithm for watermarking on compressed host data integrating channel coding and lifting based integer wavelet (Maity, 2009a). To achieve relative gain in DWR and BER performance with compression rate, we exploit the benefits of memory system, both from mathematical structure of lifting based implementation and

convolution coding. The objective is to improve simultaneously DWR and BER performance for watermark decoding against AWGN. It is also important to meet the condition that the file size of the compressed watermarked data should not increase much due to watermarking. Convolution coded compressed host data is decomposed by discrete wavelet transform using lifting to generate lossless integer wavelet coefficients. Watermark information is casted using dither modulation (DM) based QIM for ease of implementation. Experimentation is carried out on JPEG compressed data at different compression rates. The relative gain on imperceptibility and robustness performance are reported for direct watermark embedding on entropy decoded host, using repetition code, convolution code, and finally the combined use of convolution code and lifting.
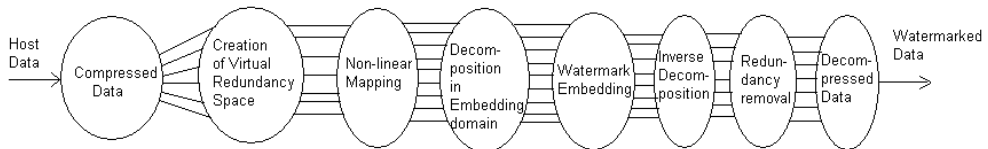

Fig. 1. Basic outline for algorithm development

3. Outline for algorithm development

The first step would be to recreate the virtual redundancy (lost due to quantization operation in compression) space on compressed data so that flexibility in data embedding is possible to regain to a certain extent. This needs the use of ECC in an intelligent way so that so called created redundancy (virtual redundancy) would not increase much the file size of the data. The other important requirement is to choose proper embedding space i.e. choice of transforms for the host image so that further data loss in QIM is protected. The choice of discrete cosine transform (DCT) and discrete wavelet transform (DWT) for decomposition of host is preferable as popular image compression of recent times like JPEG and JPEG 2000 are based on these two transforms. At the same time, one drawback for the two transforms is the results of floating-point numbers. In QIM based data embedding, it would be rounded to integer values and small values may be set to zero. Hence perfect invertibility is lost and the original input data cannot be regenerated. Another important aspect is that DCT based watermarking algorithms are robust against JPEG but not equally robust for JPEG 2000; similar argument is also valid for DWT based watermarking methods. It is seen that lifting based wavelet transform maps an integer data set into another integer data set. This transform is perfectly invertible, yields exactly the original data set and may be a potential choice for QIM watermarking on JPEG compressed data.

3.1 Integration of channel coding with integer wavelets

The convolution code is chosen here to apply on the entropy decoded compressed host data as this error-correcting code (ECC) operates on serial data and uses memory system. The use of memory system in turn creates the correlation among the sample coefficients. The Viterbi decoding is used because of highly satisfactory bit error performance, high speed of operation, ease of implementation, low cost, and fixed decoding time (Bose,2002). Again Viterbi decoding works on a bit based on either soft-decision or hard-decision. It is also reported in the digital communication literature that soft-decision decoding outperforms

over hard-decision decoding by a margin of roughly 3 dB in AWGN channels. The convolution coded data is further operated by lifting based integer wavelet transform to reduce data loss due to quantization operation for information hiding. Lifting based filtering consists of a sequence of very simple operations for which alternately odd sample values of the signal are updated with a weighted sum of even sample values and even sample values are updated with a weighted sum of odd sample values. This mathematical structure of lifting operation after applying on compressed convolution coded data creates correlation among the sample values and leads to better visual quality of watermark data. Fig. 1 shows the outline of different steps for developing general watermarking algorithm.

4. Proposed watermarking method on compressed data

The proposed watermark embedding scheme is based on the creation of virtual redundancy space on compressed data through convolution coding followed by signal decomposition through lifting based integer wavelet transform to obtain embedding space.

4.1 Watermark embedding process

Fig. 2 shows the block diagram representation of the proposed watermarking scheme. The steps are described briefly as follows:
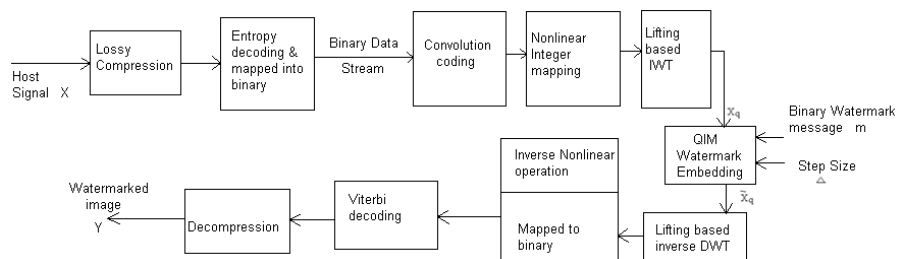

Fig. 2. Block diagram representation of watermark embedding scheme

Step 1. Entropy decoding and binary mapping

The lossy JPEG compressed host signal is first entropy decoded. The non-zero quantized DCT coefficients are then mapped to the binary data.

Step 2. Convolution coding

The binary data obtained in step 1 is then encoded using convolution coding so that each `k' bits are mapped to `t' bits where $t \leq k$.

Step 3. Non-linear mapping of encoded data

The channel coded binary data is not suitable for direct application of QIM watermarking. To create suitable quantization based embedding space, convolution coded data is then converted to integer coefficients through non-linear mapping. A simple, easily implementable and reversible such nonlinear mapping may be binary-to-decimal conversion and is used here. The binary to decimal conversion would be restricted to 8 bits/sample so that sample values remain like the pixel values of a gray scale image.

Step 4.   Decomposition using Lifting based IWT

The integer signal obtained in step 3 undergoes IWT using 5-tap/3-tap filter coefficients, however, other lifting based DWT filters can also be used. The channel coded DCT coefficients are decomposed using lifting based DWT so that watermarked signal can be simultaneously compatible to JPEG and JPEG 2000 compression operations. It is reported in watermarking literature that most wavelet-based embedding schemes are very robust against low quality JPEG 2000 compression, but are not similarly resilient against low quality JPEG compression. Similarly, DCT based digital watermarking methods are having exactly inverse characteristics for compression operations. To this aim, this method would offer certain degree of robustness against JPEG 2000 due to IWT operation applied on DCT compressed watermarked data.

Step 5.   QIM watermarking

A binary message `W' is used as watermark and two dither sequences, with length L, are generated pseudo randomly with step size (Δ) as follows:

$$d_q(0) = \{R(key) * \Delta\} - \Delta/2 , 0 \le q \le L\text{-}1 \tag{1}$$

$$d_q(1) = \begin{cases} d_q(0) + \Delta/2 \text{ if } d_q(0) < 0 \\ d_q(0) - \Delta/2 \text{ if } d_q(0) \ge 0 \end{cases} \tag{2}$$

Where R (*key*) is a random generator. The q-th watermarked wavelet coefficients S_q is obtained as follows:

$$S_q = \begin{cases} Q\{X_q - d_q(0), \Delta\} + d_q(0) \text{ if } W'(i,j) = 0 \\ Q\{X_q + d_q(1), \Delta\} - d_q(1) \text{ if } W'(i,j) = 1 \end{cases} \tag{3}$$

where X_q is the convolution coded q-th IWT coefficients of the compressed host data, Q is a uniform quantizer (and dequantizer) with step Δ, and W(i,j) is the (i,j) -th pixel of the watermark.

Step 6.   Watermarked image formation

Inverse integer wavelet transform (IIWT) is then applied on the watermarked coefficients. Inverse non-linear operation i.e decimal to binary conversion maps each integer signal into binary data. The Viterbi decoding is then applied on the binary data to map each t-bits into k bits. This operation is done for the inverse operation of channel coding used as convolution codes i.e. for redundancy removal and not for watermark decoding. Thus entropy decoded watermarked data is obtained. This watermarking process may be analogous to `hidden QIM' as the information embedding process shown in Fig. 1 and Fig. 2 consists of (i) preprocessing of the compressed host data using convolution coding, non-linear mapping, IWT operation (2) QIM embedding, and (3) post processing using convolution decoding, inverse non-linear mapping, and IIWT to form the composite signal (Chen & Wornell, 2001).

4.2 Watermark decoding process

The watermark decoding is done from the compressed watermarked image. Entropy decoding of compressed watermarked data is done first followed by binary mapping. Then

again convolution coding with proper code rate followed by non-linear mapping are done as it was performed during watermark embedding. Integer wavelet coefficients for watermarked data are then used for watermark extraction. Fig. 3 shows block diagram representation of watermark decoding process.
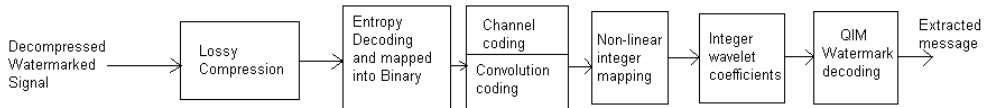

Fig. 3. Block diagram representation of watermark decoding scheme

The watermark information can be extracted from the compressed data using the following rule.

$$A = \sum_{q=0}^{L-1} (\,|\,Q(Y_q - d_q(0), \Delta) + d_q(0) - Y_q\,|\,)$$

$$B = \sum_{q=0}^{L-1} (\,|\,Q(Y_q + d_q(1), \Delta) - d_q(1) - Y_q\,|\,) \tag{4}$$

where Yq is the q-th IWT coefficient (possibly noisy due to transmission channel or any attack operation applied on the watermarked data) of the watermarked data. The symbols A and B are the decision variables used for extraction of watermark bits. A watermark bit W(i,j) is decoded using the rule: where Yq is the q-th IWT coefficient (possibly noisy due to transmission channel or any attack operation applied on the watermarked data) of the watermarked data. The symbols A and B are the decision variables used for extraction of watermark bits. A watermark bit W(i,j) is decoded using the rule:

$$W'(i,j) = \begin{cases} 0 & \text{if } A < B \\ 1, & \text{otherwise} \end{cases} \tag{5}$$

5. Performance evaluation

Performance of the proposed watermarking method is studied in terms of change in DWR with the change in watermark power as well as robustness performance as measure of BER for watermark decoding against AWGN. We have extensively studied the performance for direct watermarking on entropy decoded DCT coefficients, using repetition codes and convolution codes with code rate R=1/2, 1/4, 1/6. The experimentation has been carried out for large number of JPEG compressed images with different compression rates, however, we report here results for quality factor 60.

Fig. 4 (a)-(c) show some benchmark test images (petitcolas) Lena, Boat and Perrer of size (256x 256), 8 bit/pixel gray scale image and Fig. 4(d) shows a visually recognizable binary watermark of size (32x 32). The binary watermark size so chosen would allow embedding of single watermark bit in each (8x 8) block of the host image. The present study uses peak-signal-to-noise-ratio (PSNR) (Gonzalez & Woods, 2005) and mean structural similarity index measure (MSSIM)(Wang et al., 2004) to quantify the visual quality of the watermarked image with respect to the host image.
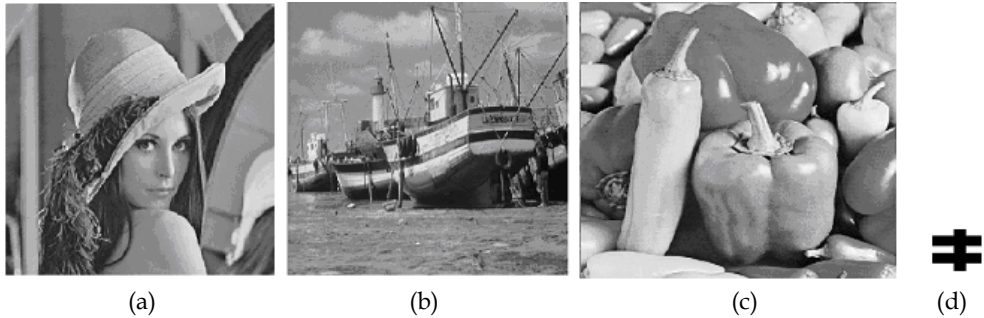
Fig. 4. Original or host image (a)Lena (b) Boat (c) Pepper (d) Binary watermark

First of all we would present the effect of different watermark powers on relative quality of the watermarked images. Fig. 5 (a)-(e) show the watermarked images obtained after data embedding on entropy decoded DCT coefficients at various watermark powers determined by the different step sizes of the quantization operation used for QIM. The watermark powers are set at 12.73 dB, 14.31 dB, 15.22 dB, 16.05 dB and 16.81 dB for Fig. 5(a), 5(b), 5(c), 5(d) and 5(e), respectively. The corresponding PSNR values for the watermarked images are 36.89 dB, 35.59 dB, 34.84 dB, 34.09 dB and 33.42 dB, respectively, while corresponding MSSIM values for them are 0.9388, 0.9197, 0.9068, 0.8920 and 0.8767, respectively. The watermark power (Boyer et al, 2006) is defined as:

$$WP = 10 \ \log_{10} \frac{\Delta^2}{12} \ dB \qquad\qquad (6)$$

Fig. 5. Watermarked images after embedding on entropy decoded DCT coefficients at watermark power (a) 12.73 dB, (b) 14.31dB (c) 15.22 dB (d) 16.05dB (e) 16.81dB

Fig. 6(a)-(e), Fig. 7(a)-(e), and Fig. 8(a)-(e) show the different watermarked images with watermark powers at 12.73 dB, 14.31 dB, 15.22 dB, 16.05 dB and 16.81 dB, respectively and with convolution coding rate R=1/2, 1/4 and 1/ 6, respectively. The symbols P and M associated with each figure indicate PSNR values in dB and MSSIM values, respectively. Similarly, Fig. 9(a)-(e), Fig. 10(a)-(e) and Fig. 11(a)-(e), show the different watermarked images with watermark powers at 12.73 dB, 14.31 dB, 15.22 dB, 16.05 dB and 16.81 dB, respectively and with the combined use of IWT and convolution coding on entropy decoded DCT coefficients at coding rate R=1/ 2, 1/ 4 and 1/ 6, respectively.

(P=40.75,M=0.9762) (P=40.31,M=0.9731) (P=40.02,M=0.9714) (P=39.96,M=0.9713) (P=39.69,M=0.9697)
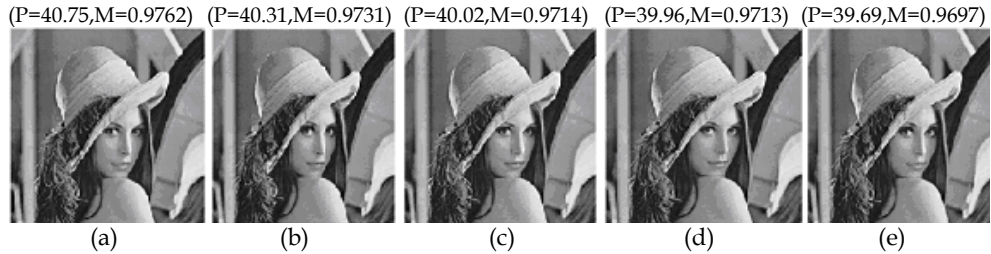

(a) (b) (c) (d) (e)

Fig. 6. Watermarked images after embedding on entropy decoded DCT coefficients with convolution coding rate 1/2 at watermark power (a) 12.73dB (b)14.31 dB, (c) 15.22 dB, (d) 16.05 dB, (e)16.81 dB
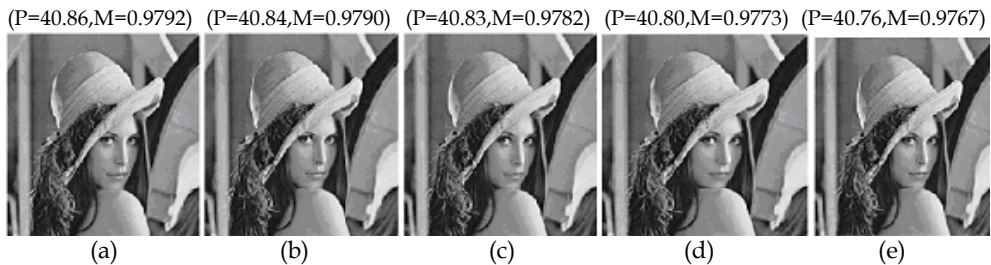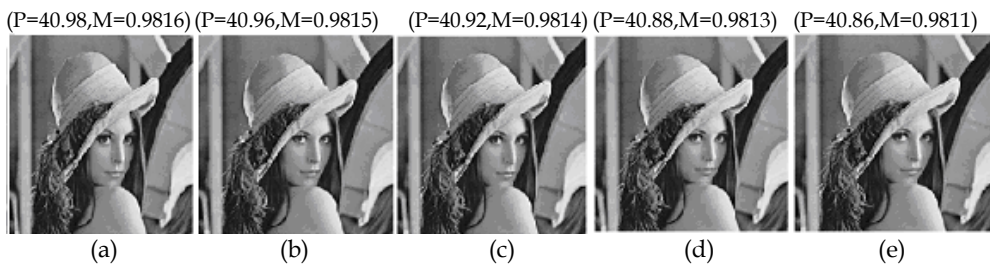
(P=40.86,M=0.9792) (P=40.84,M=0.9790) (P=40.83,M=0.9782) (P=40.80,M=0.9773) (P=40.76,M=0.9767)

(a) (b) (c) (d) (e)

Fig. 7. Watermarked images after embedding on entropy decoded DCT coefficients with convolution coding rate 1/4 at watermark power (a) 12.73dB (b)14.31 dB, (c) 15.22 dB, (d) 16.05 dB, (e)16.81 dB

(P=40.98,M=0.9816) (P=40.96,M=0.9815) (P=40.92,M=0.9814) (P=40.88,M=0.9813) (P=40.86,M=0.9811)

(a) (b) (c) (d) (e)

Fig. 8. Watermarked images after embedding on entropy decoded DCT coefficients with convolution coding rate 1/6 at watermark power (a) 12.73dB (b)14.31 dB, (c) 15.22 dB, (d) 16.05 dB, (e)16.81 dB

(P=41.23,M=0.9851)   (P=41.20,M=0.9847)   (P=41.19,M=0.9825)   (P=41.16,M=0.9823) (P=41.12,M=0.9821)

    (a)   (b)   (c)   (d)   (e)

Fig. 9. Watermarked images after embedding on entropy decoded DCT coefficients with integer wavelets and convolution coding rate 1/2 at watermark power (a) 12.73dB (b)14.31 dB, (c) 15.22 dB, (d) 16.05 dB, (e)16.81 dB
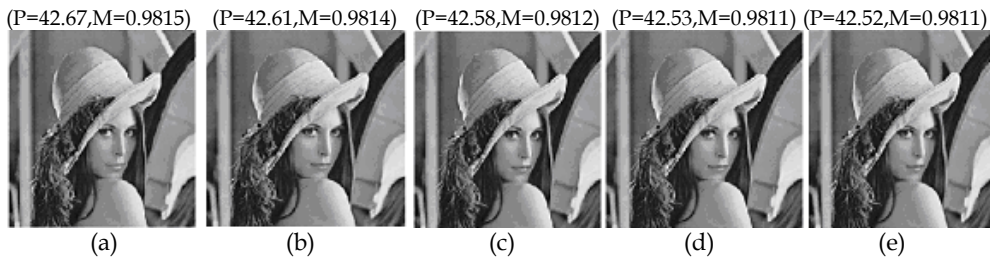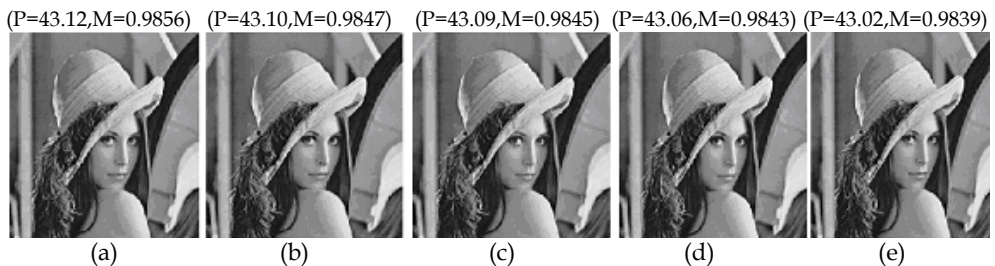
(P=42.67,M=0.9815)   (P=42.61,M=0.9814)   (P=42.58,M=0.9812)   (P=42.53,M=0.9811) (P=42.52,M=0.9811)

    (a)   (b)   (c)   (d)   (e)

Fig. 10. Watermarked images after embedding on entropy decoded DCT coefficients with integer wavelets and convolution coding rate 1/4 at watermark power (a) 12.73dB (b)14.31 dB, (c) 15.22 dB, (d) 16.05 dB, (e)16.81 dB

(P=43.12,M=0.9856)   (P=43.10,M=0.9847)   (P=43.09,M=0.9845)   (P=43.06,M=0.9843) (P=43.02,M=0.9839)

    (a)   (b)   (c)   (d)   (e)

Fig. 11. Watermarked images after embedding on entropy decoded DCT coefficients with integer wavelets and convolution coding rate 1/6 at watermark power (a) 12.73dB (b)14.31 dB, (c) 15.22 dB, (d) 16.05 dB, (e)16.81 dB

We have also studied DWR vs watermark power performance for the repetition code at different coding rates and performance comparison for convolution code and repetition codes are shown graphically in Fig. 11. In the figure, repetition codes is denoted as Rep. and convolution codes as Con. with different code rates. Fig.13 shows the similar comparison of DWR using channel coding and IWT coefficients using lifting (denoted as Lift. in the graphs as it is generated by lifting scheme). It is quite clear from both the graphs that significant improvement in DWR is achieved due to the use of convolution coding compared to the direct embedding of watermark information on the entropy decoded coefficients. The improvement

is found to be higher in case of convolution codes compared to the repetition codes. The use of integer wavelet coefficients in both cases show relative improvement in DWR of the order of ~ 0.75 dB but benefits in other way. A careful inspection on Fig. 12 and Fig. 13 show that the use of integer wavelet coefficients with channel coding, particularly for convolution coding, maintains high DWR values even with large increase in watermark power leading to a significant improvement in BER performance against AWGN attack. The overall high DWR value is achieved due to convolution coding which is further augmented through the correlations among the sample coefficients due to the use of lifting. In other words, large value of step sizes (Δ) can be selected even with maintaining high DWR. This large watermark power improves BER performance greatly against AWGN attack leading to better robustness.

The above observation for robustness improvement is further supported by BER performance shown in Fig. 14 and is also explained mathematically by Eq. (7). BER is mathematically indicated by probability of bit error P_b in watermark detection. The more general expression for P_b in case of M-PAM (M-pulse amplitude modulation) signaling (Voloshynovskiy& Pun, 2002), is expressed as

$$P_b = \frac{2(M-1)}{M} \, \gamma \, (\sqrt{\frac{Nd_0^2}{4\sigma_x^2}}) \tag{7}$$

where M corresponds to M-PAM (for the present case M=2), N is the gain in code rate in terms of the number of host sample points over which each watermark bit is embedded, d_0^2 indicates the watermark power, γ (.) indicates the complementary error function and σ_x^2 is
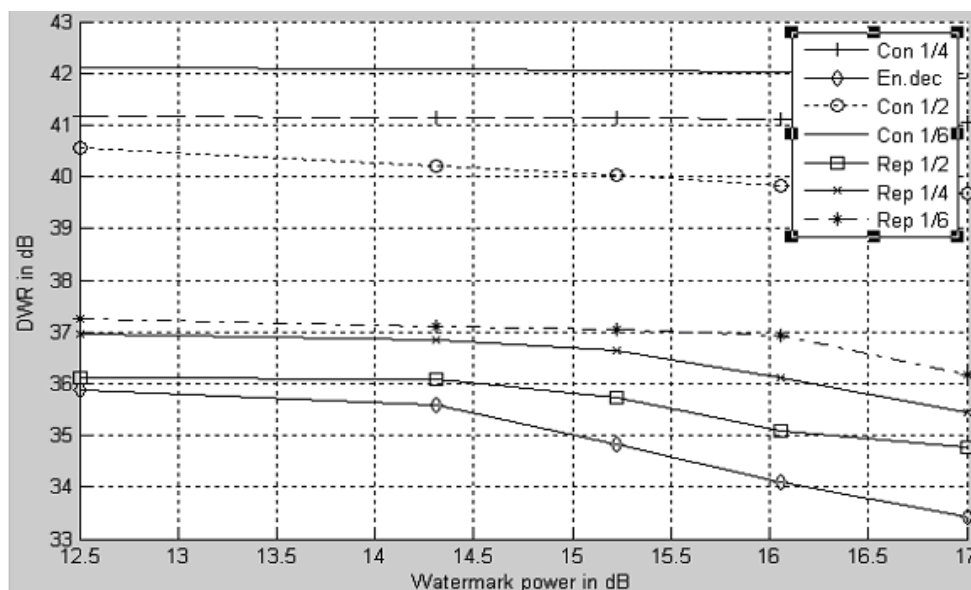

Fig. 12. DWR vs watermark power for direct embedding on entropy decoded data and using channel coding, namely convolution coding and repetition coding
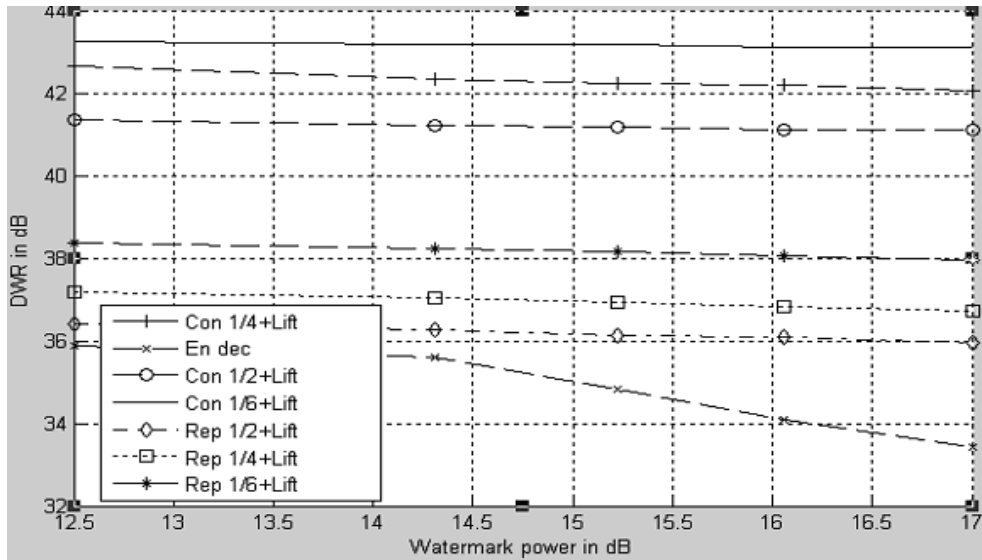
Fig. 13. DWR vs watermark power for direct embedding on entropy decoded data and using both channel coding and lifting
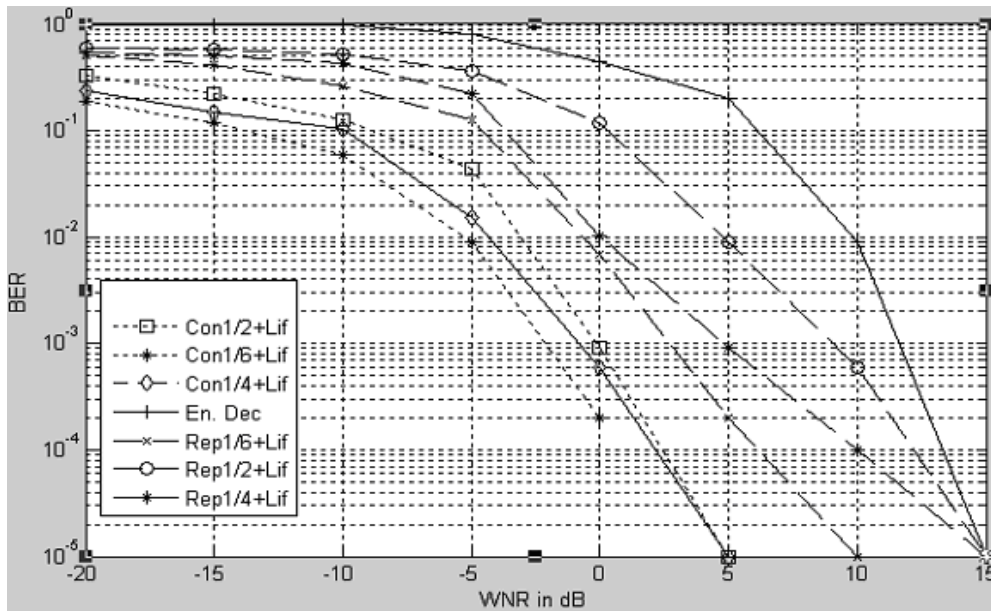

Fig. 14. BER performance at different watermark- to-noise (WNR) in dB

the variance of the embedding coefficients. It is seen from the simulation results over large number of images and shown in Table 3 that the variance values of the IWT coefficients are much lower than the similar for DWT coefficients. This low variance in turn leads to the reduction in P_b values for the former compared to the latter. BER Performance for watermarking on entropy coded data is poor as in such case N=1 and σ_x^2 is high. On the other hand, low P_b value for the decoded watermark in the proposed system is achieved due to two-fold advantages, namely large N-values due to code rates and low σ_x^2 value compared to normal DWT coefficients.

To test the robustness of the proposed scheme, some typical signal processing operations, such as filtering, sampling, histogram equalization, various noise addition, dynamic range change, and lossy JPEG compression are performed on watermarked image. Robustness performance is also tested against shifts, different rotations, and other geometric attacks like affine transformation, since QIM-based schemes reported in the literature show relatively inferior performance for such kind of operations. The subsequent simulation results are reported here after applying various operations over watermarked images obtained by combined use of convolution coding at rate R=1/ 6 and integer wavelets, at quality factor 60 and watermark power 12.73 dB. The associated quantitative measures for the watermarked images are ~ 40.98 dB (PSNR) and ~ 0.9816 (MSSIM) before applying any attack operation. For image scaling operation, before watermark extraction, the attacked images are rescaled to the original size. For rotation operation, the rotation angles undergone by the watermarked images are estimated by control point selection method with the help of the original images. The rotated watermarked images are then inverse rotated and are corrected by linear interpolation. Now those corrected watermarked images are used for watermark detection. This is done to compensate for the effect of loss in data due to the rotation operation. The experimental results of robustness against various image processing operations are shown in Table 1. It is seen that proposed algorithm can successfully resist attacks like filtering, scaling, cropping, random removal of some rows and columns, combination of scaling and small rotation. The visual quality of the extracted watermark is quantified by normalized cross correlation (NCC) as defined below

$$NCC = \frac{\sum_i \sum_j w_{ij} w'_{ij}}{\sum_i \sum_j w_{ij}^2} \qquad (8)$$

Where, $1 \le (i,j) \le n$ and w_{ij} and w'_{ij} are the binary pixel values at the position (i,j) of the embedded and extracted watermarks, respectively.

Fig. 15(a) and Fig. 15(c) show the watermarked images with DWR 21.41 dB and 24.03 dB, respectively obtained after spatial mean and median filtering operations using window sizes (11x11). The corresponding extracted watermark images are shown in Fig. 15(b) and 15(d), respectively with NCC values 0.9816 and 0.9911, respectively. Fig. 15(e) shows significantly improved robustness performance for the present scheme compared to (Huang, 2007;Wu et al., 2005) method against JPEG compression operation. In all three cases, watermark power is set to 12.73 dB and watermark size is (32 x 32).
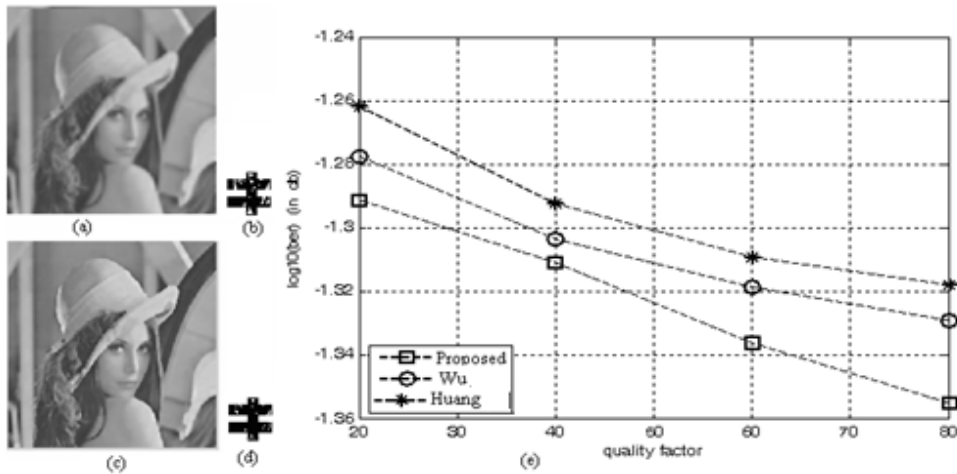
Fig. 15. (a), (c): Watermarked images after mean and median filtering, respectively, (b)and(d): Extracted watermarks from (a), and (c), respectively, (e) Robustness performance comparison against JPEG compression

Name of attack	Strength	PSNR in dB	MSSIM value	NCCvalue
Lowpassfiltering	3x3	28.70	0.89	0.98
Highpassfiltering	3x3	20.36	0.95	1.00
Down and upsampling	0.9	35.45	0.96	1.00
	0.75	34.12	0.95	1.00
	0.5	30.32	0.95	0.87
Cropping	13%	11.09	0.75	1.00
	52%	8.32	0.51	1.00
Rotation	90	45.21	0.98	1.00
	17	15.66	0.86	0.95
	60	14.01	0.82	0.87
Dyn. range change	(50-200)	22.23	0.85	1.00
Salt & Peppre Noise	0.01	24.42	0.75	0.96
	0.03	19.67	0.47	0.92
	0.05	17.44	0.32	0.87
Speckle Noise	0.01	25.31	0.54	0.97
	0.03	20.10	0.36	0.89
	0.05	17.50	0.28	0.83
Gaussian Noise	0.01	19.00	0.25	0.94
	0.03	18.70	0.24	0.83
	0.05	18.08	0.24	0.79

Table 1. Robustness performance against various image processing operations for the proposed method at quality factor 60; PSNR and MSSIM values for the watermarked images are ~ 40.98 dB and ~ 0.9816 (MSSIM), respectively before applying any attack operation

Performance of the proposed algorithm is also studied for gray scale watermark image. We consider a 4-bits/pixel gray image of size (16×16) as watermark and (512×512), 8 bits/pixel gray images, as host image. The gray scale watermark image is now converted into bit string. An extended binary string is then developed by employing variable redundancy in different bit planes of the gray scale watermark image. The variable redundancy is accomplished by incorporating more number of bits in higher order bit plane and less or no redundancy for lower order bit plane. The reason is that the higher order bit planes contain the majority of the visually significant data and needs more protection in watermarking. On the other hand, lower bit planes contribute to more subtle details in the image. In the present case, MSB i.e. 4th bit of pixel value is repeated nine (9) times, 3rd bit five (5) times, and no redundancy for the remaining two LSBs. Thus a single 4bits/ pixel now becomes as 16 bits. The length of the 4bits/pixel (16x16) gray scale watermark image thus becomes an equivalent binary watermark of size (64x64). The host image of size (512x512) then embeds (64x64) watermark, where each (8x8) block would embed one watermark bit. The binary watermark is first extracted. Then each watermark substring of length 16 is partitioned into four segments of length 9, 5, 1 and 1. A decision of bit '1' or '0' is made for both sub strings of length nine (9) and five (5), based on majority decision, in accordance with the watermark image encoding rule. The scheme is identical to the use of error correction code controlled by Hamming distance.

Fig. 16(a) shows (512x512) Lena image and Fig. 16(b) is a (16x16), 4bits/pixel gray scale watermark image (although looks binary but it is a gray scale watermark image of 4bits/pixel) and Fig. 16(c) shows watermarked images after embedding on entropy decoded
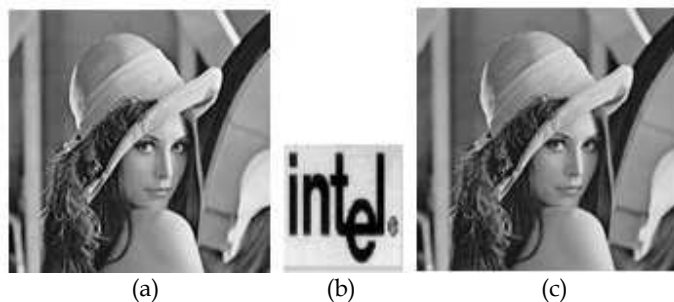

Fig. 16. (a) Host image Lena (512 x512) (b)4 bits/pixel gray scale watermark of size (16x16) (d): Watermarked image
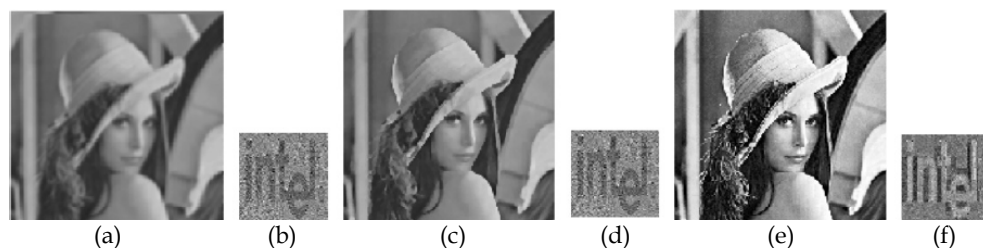

Fig. 17. (a), (c): Watermarked images after mean and median filtering, respectively, (b) and (d): Extracted watermarks from (a), and (c), respectively, (e) watermarked image after histogram equalization, (f) extracted watermark from Fig. (e).

DCT coefficients with integer wavelets and convolution coding rate 1/6 at watermark power 12.73dB. The PSNR and MSSIM values for the watermarked image are 37.25 dB and 0.93, respectively. Fig. 17 (a) and (b) show the watermarked image after mean filtering (21.41dB) with size (11x11) and extarcted watermark, respectively. Fig. 17(c) and (d) show the watermarked image after median filtering (24.03 dB) with window size (9 x9) and the extracted watermark, respectiley. Finally, Fig. 17(e) and (f) shows the watermarked image (19.42 dB) after histogram equalization and the corresponding extracted watermark, respectively. In all cases, extracted watermark images are visually recognizable and indicate the robustness of the proposed scheme.

The proposed algorithm, although presented for gray scale images, can easily be extended for color images by considering each color channel as a gray-scale image. There are several ways to represent color images numerically, for example: RGB, YC_bC_r, CMY. The symbolsR, G, B, Y, C_b and C_r denote the red, the green, the blue, the luminance, the chrominance-blue and the chrominance-red, respectively while C, M and Y indicate cyan, magenta, and yellow, respectively. The CMY format is preferably used in printing industry and color images are most commonly represented in RGB format. In RGB format, the image is composed of three component planes; red, green, and blue color components. When the discrete cosine transformation is applied, each color component is transformed independently. Researchers have reported that for some typical applications, such as image compression, the RGB color space is not optimal. It turns out the human brain is more attuned to small changes in terms of luminance and chrominance (i.e. chrominance blue and chrominance red). A luminance channel carries information regarding the brightness of a pixel. Chrominance is the difference between a color and a reference channel at the same brightness. The most common of these spaces and the one used by JPEG2000 is the YC_bC_r space. The Y channel is luminance, while C_b and C_r are chrominance channels. Moreover, Y, C_r and C_b color components are less statistically dependent than R, G and B color components, and hence, they can be processed independently leading to better compression. The watermarks can then be embedded in appropriate color channels.

Finally, we also like to highlight simplicity of digital circuit design for the implementation of IWT of the filter coefficients, which is one of our future research work for the proposed algorithm. The multiplication operations may be carried out using simple shift-and-add multiplier blocks. Since multiplicands are signed, 2's complement arithmetic can be used in all mathematical operations. It is observed that the denominators of the coefficients are expressed in power of 2. Hence the division operation can easily be accomplished using parameterized right shifter blocks. Thus a right shifter block tailing every multiplier unit would be used in the filter bank design. The circuit of decimation (down-sampling) and interpolation (up-sampling) can be realized using D type flip-flop. In the decimator, a D flip-flop would be used and the clock rate of the input must be equal to half the clock rate of the D flip-flop so that only every alternate input to the decimator is fed to the interpolator unit. The clock rate of the input to the latter must be equal to twice that of the clock for the D flip-flop so that a zero would be inserted between every two successive inputs to the up-sampling block. This simplicity in hardware design makes this algorithm attractive for application specific integrated circuit (ASIC) or field programmable gate array(FPGA) based real-time implementation (Maity et al, 2009b).

## 6. Conclusions and scope of future works

A novel QIM watermarking is proposed using channel coding and lifting while channel coding is applied on host compressed data unlike conventional encoding of the watermark itself. Channel coding essentially creates a virtual redundancy space on compressed data to obtain flexibility in watermarking without increasing the file size of the compressed data. Channel coding offers improvement both for imperceptibility as well as BER performance while lifting contributes much on BER performance. Simulation results show that 6.24 dB (9.50 dB) improvement in DWR for watermark power at 12.73 dB (16.81 dB) and 15 dB gain in noise power for watermark decoding at BER of 10^{-2} are achieved, respectively over direct watermarking on entropy decoded data.

Future works may be carried out to design capacity optimized hidden watermarking scheme on the compressed data using non-zero and zero coefficients, as the latter may easily be mapped to non-zero coefficients using channel coding. Some widely used soft computingtool like Genetic Algorithms (GAs) may be explored for this optimization work. An extension of the proposed work may be to design VLSI chip using ASIC or FPGA, as standard JPEG compression, channel coding, lifting and nonlinear mapping used in this work can easily be mapped in hardware platform.

7. References

Allatar, A. M.; Lin E. T. & Celik, M. U. (2003). Watermarking Low Bit-rate Advanced Simple Profile MPEG-4 Bitstreams, *IEEE Trans. on Circuits and Systems for Video Tech.*, Vol.13,787-800.

Bose, R. (2002) *Information theoy coding and crypography*, Tata McGraw-Hill.

Boyer, J. P.; Duhamel, P. J. & Blanc-T, Asymptotically optimal scalar quantizers for QIM watermark detection. *Proc. IEEE ICME*, pp 1373-1376.

Chen, B. & Wornell, G. W. (2001). Quantization index modulation: a class of provably good methods for digital watermarking and information embedding. IEEE Trans. on Information Theory, Vol. 47, 1423- 1443.

Choi, Y. & Aizawa, K. (200). Digital watermarking using inter-block correlation: extension to JPEG coded domain, *Proc. IEEE Int. Conf. Information Technology: Coding andComputing*, pp. 133-138.

Elbasi, E. (2007). Robust MPEG Video watermarking in wavelet domain. Trakya Univ. Jour. Sci, Vol. 8, 87-93.

Fridrich, J; Goljan, M., Chen, Q., & Pathak, V. (2004). Lossless data embedding with file size preservation, Proc. EI, Security, Steganography, Watermarking Multimedia Contents VI, SPIE, Vol.5306, pp. 354-365.

Gonzalez, R. C. & Woods, R. E. Digital image processing, Pearson Education, New Delhi, India.

Hartung, F. & Kutter, M. (1999). Multimedia Watermarking Techniques, Proc. IEEE, Vol. 87, 1079--1107.

Huang, H-Y.; Fan, C-H. & Hsu, W.-H.(2007). An effective watermark embedding algorithm for high JPEG compression, Proc. of IAPR Conference on Machine Vision Applications, pp. 256-259.

Karakos, D. & Papamarcou, A. (2003). A relationship between quantization and watermarking rates in the presence of additive Gaussian attacks, IEEE Trans. on Information Theory, Vol. 49,1970-1982.

Langelaar, G. C.; Setyawan, I. & Lagendijk, R. L. (2000). Watermarking digital image and video data, IEEE Signal Process. Mag., Vol. 17, 20-46.

Luo, W.; Heileman, G. L. & C. E. Pizano.(2002). Fast and robust watermarking of JPEG files, Proc. IEEE 5th Southwest Symp. Image Analysis and Interpretation, pp. 158-162.

Maity, S. P.; Delpa, C., Braci, S., Boyer, R. (2009a). Hidden QIM watermarking on compressed data using channel coding and lifting, Proc. of third Int. Conf. on Pattern Recognition and Machine Intelligence, Vol. 5909, pp. 414-419.

Maity, S. P.; Kundu, M. K. & Maity, S. (2009b). Dual purpose FWT domain spread spectrum image watermarking in real-time, Special issues: circuits & systems for realtime security & copyright protection of multimedia, Journal of Computers & Electrical Engg., Elsevier, Vol.35, 415-433.

Maity, S. P.; Phadikar, A. & Kundu, M. K. Image error concealment based on QIM data hiding in dual-tree complex wavelets, International Journal of wavelets, Multiresolution and Information Processing (Article in press).

Maor, A. & Merhave, N. (2004). On joint information embedding and lossy compression, Proc. of IEEE Int. Symp. On Info. Th., pp. 194.

Maor, A. & Merhave, N.(2005). On joint information embedding and lossy compression in the presence of a stationary memoryless attack channel, EEE Trans. on Info. Th., Vol. 51, 3166-3175.

Mobasseri, B. J. & Berger, R. J. (2005). A foundation for watermarking in compressed domain, IEEE Signal Processing Letter, Vol.12, 399-402.

Nakajima, K. & Tanaka, K. (2005). Rewritable data embedding on MPEG coded data domain, IEEE Proc. of ICME, pp. 682- 685.

F. A. P. Petitcolas. (2000). Watermarking schemes evaluation, IEEE Signal Proc. Mag., Vol.17, 58-64.

Taniguchi, M. (2005). Scaling detection method for watermarked MPEG content, Proc. IEEE Int. Conf. Image Proc., Vol. 1, pp. 225-228.

Voloshynovskiy, S. & Pun, T. (2002). Capacity security analysis of data hiding technologies, Proc. IEEE International Conference on Multimedia and Expo, pp. 477--480.

Wang, Z.; Bovik, A. C., Sheikh, H. R., Simoncelli, E.P. (2004). Image quality assessment: from error measurement to structural similarity, IEEE Transactions on Image Processing, Vol. 3, 1--14.

Wong, P. H. W. & Au, O. C. (2000). Data hiding and watermarking in JPEG compressed domain by DC coefficient modification, Proc. SPIE Security and Watermarking of Multimedia Contents, Vol. 3971, pp. 237-244.

Wong, P. H. W. & Au, O. C. (2001). Data hiding technique in JPEG compressed domain, Proc. of SPIE Security and Watermarking of Multimedia Contents, Vol. 4314, pp. 309--320.

Wu, G. & Yang, H. (2005). Joint watermarking and compression using scalar quantization for maximizing robustness in the presence of additive Gaussian attacks, IEEE rans. on Signal Processing, Vol. 53, 834-844.
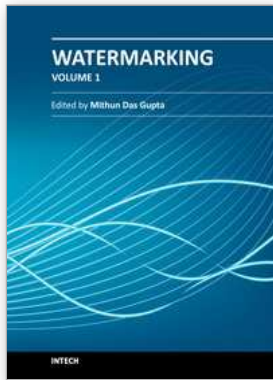
Watermarking - Volume 1

Edited by Dr. Mithun Das Gupta

This collection of books brings some of the latest developments in the field of watermarking. Researchers from varied background and expertise propose a remarkable collection of chapters to render this work an important piece of scientific research. The chapters deal with a gamut of fields where watermarking can be used to encode copyright information. The work also presents a wide array of algorithms ranging from intelligent bit replacement to more traditional methods like ICA. The current work is split into two books. Book one is more traditional in its approach dealing mostly with image watermarking applications. Book two deals with audio watermarking and describes an array of chapters on performance analysis of algorithms.

How to reference

In order to correctly reference this scholarly work, feel free to copy and paste the following:

INTECH
open science | open minds